DEUTSCHES ELEKTRONEN-SYNCHROTRON DESY

DESY SR-77/18
November 1977

Vacuum Ultraviolet Reflectivity and Band Structure of $SrTiO_3$ and $BaTiO_3$

by

D. Bäuerle and W. Braun
Fachbereich Physik, Universität Osnabrück

V. Saile
Sektion Physik, Universität München

G. Sprüssel
Institut für Experimentalphysik, Universität Kiel

E. E. Koch
Deutsches Elektronen-Synchrotron DESY, Hamburg

NOTKESTRASSE 85 · 2 HAMBURG 52

To be sure that your preprints are promptly included in the
HIGH ENERGY PHYSICS INDEX ,
send them to the following address (if possible by air mail) :

DESY
Bibliothek
Notkestrasse 85
2 Hamburg 52
Germany

Vacuum Ultraviolet Reflectivity and Band Structure of $SrTiO_3$ and $BaTiO_3$

by

D. Bäuerle and W. Braun

Fachbereich Physik, Universität Osnabrück

Federal Republic of Germany

and

V. Saile

Sektion Physik, Universität München,

and

G. Sprüssel

Institut für Experimentalphysik, Universität Kiel,

and

E.E. Koch

Deutsches Elektronensynchrotron DESY, Hamburg

Abstract

The room temperature near-normal incidence reflectance spectra for $SrTiO_3$ and $BaTiO_3$ have been measured in the energy region 10 to 32 eV. The optical constants for the region 0 to 32 eV have been derived from a Kramers-Kronig analysis by including earlier measurements for the low energy region. For $SrTiO_3$ five peaks in the Ti3d derived conduction band density of states have been found on the basis of experimental data only, neglecting excitonic effects. The energies of these peaks are in excellent agreement with peaks in the density of states calculated by Mattheiss. The results for $BaTiO_3$ could not be interpreted as unambiguously in such a scheme. Below the onset of core to conduction band transitions, evidence for core level excitons has been found for both $SrTiO_3$ and $BaTiO_3$.

I. Introduction

During the last years oxidic perovskites have found increasing interest in connection with ferroelectricity (1), superconductivity (2) and catalysis (3). Together with these problems and others, the question for a better knowledge of the band structure of these materials did arise. Band structure calculations by various authors (4-11) were mainly compared with optical spectra obtained by normal incidence reflectance (12, 13) or by the electroreflectance method (14). However, these investigations only covered the range up to 10 - 15 eV. Recently, the density of valence states of $SrTiO_3$ and $BaTiO_3$ was investigated by X-ray photoelectron spectroscopy (XPS) (15, 16). In addition, core levels have been studied in the binding energy range from -10 to -40 eV (15) and the range -10 to -80 and -520 to -535 eV (16). The binding energies are referred to the top of the valence band (TVB).

In this paper we report on near - normal incidence reflectance spectra (angle of incidence 7.5^{o}) in the photon energy range 10 to 32 eV. The polarized synchrotron light from the storage-ring DORIS at Hamburg was monochromatized with a high resolution monochromator described elsewhere (17). Polished single crystals of $SrTiO_3$ and $BaTiO_3$ (100 faces in the cubic phase) were inserted into the ultrahigh vacuum chamber without further treatment. The $BaTiO_3$ sample was not poled because the effect of tetragonality on the band structure was found to be small (10, 12).

II. Results

Figs. 1 and 2 show the room temperature reflectivity spectra of $SrTiO_3$ and $BaTiO_3$ in the photon energy region 0 to 32 eV. Our data, which start at about 10 eV, were adapted in the region of overlap to the low energy spectra measured by Cardona (12). Transitions from the valence to the conduction bands dominate the spectra from the onset of intense absorption (3.4 eV for $SrTiO_3$ and 3.2 eV for $BaTiO_3$) up to about $h\nu$ = 15 eV and $h\nu$ = 13 eV for $SrTiO_3$ and $BaTiO_3$, respectively. Superimposed on the tail of these valence to conduction band transitions one observes at higher energies structure which has to be associated with transitions originating from the Sr 4p, Ba 5p and O 2 s outer core levels. Intense broad reflection bands centered at about 28 eV for $SrTiO_3$ and 23 eV for $BaTiO_3$ are observed. Single peaks or shoulders in the spectra are labelled by "A" and "B" for $SrTiO_3$ and $BaTiO_3$, respectively. The energies of these structures are listed together with the energies of similar structures in the region 1 - 10 eV, measured by Frova and Boddy (14), in Tables 1 and 2. In parantheses the labelling of peaks used by Cardona (12) and Frova and Boddy (14) are also included in the Tables.

In order to obtain the optical constants from the data in Figs. 1 and 2 a Kramers-Kronig analysis was performed by using the program of Klucker and Nielsen (18), and assuming a decrease of the reflectivity by ω^{-4} for energies $h\nu > 32$ eV. The results for the real- and imaginary part of the dielectric function are shown in Figs. 3 and 4. In the low energy region, our results for ε_1 and ε_2 are in reasonable agreement with those calculated by Cardona (12). We note, that the structures listed in Tables 1 and 2 occur at about the same energies in the ε_2 data. Thus the original reflectivity

data will be used for further discussion. There is one striking difference between the reflectivity spectra and the ε_2-spectra. The latter do not show structure in the broad range of high reflectivity near 28.5 eV and 23.1 eV for $SrTiO_3$ and $BaTiO_3$, respectively. In these regions from 26.3 to 29.1 eV and 22.2 to 25.5 eV for $SrTiO_3$ and $BaTiO_3$ the ε_1-curves exhibit negative values, while the ε_2-curves show a gradual decrease indicating exhaustion of the oscillator strengths for transitions originating from the Sr 4p, Ba 5p and O2s levels.

In Figs. 5 and 6 the loss function, $-\mathrm{Im}\left(\frac{1}{\varepsilon}\right)$, the absorption coefficient, μ, and the real, n, and imaginary part, K, of the refractive index are plotted for $SrTiO_3$ and $BaTiO_3$. The loss functions for both materials show intense maxima at 29.7 eV for $SrTiO_3$ and at 27.3 eV for $BaTiO_3$ due to the excitation of plasmons.

IV. Discussion

A. Correlation of Transitions

In earlier papers it was shown that the comparison of the experimental data and the band structure calculations did not yield satisfactory agreement (12, 15). Therefore, we first try to classify the observed transitions on the basis of experimental data only. From the XPS data (15) we take the energies of the O2s, Sr4p, $Ba5p_{1/2}$, and $Ba5p_{3/2}$ core levels, and the maxima in the density of the O2p derived valence states; the corresponding energies are listed in Table 3. If we assume that the initial states of observed transitions are the levels listed in Table 3 including the top of the valence band TVB, we obtain together with the data listed in Tables 1 and 2 a plausible classification as given in Fig. 7. Thus in a simple atomic picture most of the observed transitions can be

correlated with transitions from valence or core states, by assuming empty energy levels L_o, L_1, L_2, L_3, L_4, and L_1, L_2, L_3 above the TVB for $SrTiO_3$ and $BaTiO_3$, respectively. In addition, for explaining the energy of the "doublet" A_{15}, A_{16} in Fig. 1, a spin orbit splitting of the Sr4p level of about 0.6 eV was assumed. Such a splitting is beyond the limit of resolution in the XPS spectra (19), and was therefore not observed in these data. The value of 0.6 eV is however in good agreement with the value of 0.5 eV, given for Sr^{2+} by Herman and Skillman (20) (see also the calculation as reported in (21)).

The positions of levels L_i are in the energy range of Ti3d levels. This means that in this simple picture transitions A_{17} and B_{20} are dipole forbidden. This may explain the low intensity of peak B_{20} in the reflectivity or ε_2 data. The "strong" structure A_{17} could be alternatively explained as due to transitions from Sr4p levels to L_4. The remaining structures, A_{10} and A_{11} for $SrTiO_3$ and B_{10}, B_{11}, B_{18}, B_{19}, B_{21} for $BaTiO_3$ do not fit into this scheme. This is not surprising since final states in addition to the Ti3d levels arising for instance from Sr4d, Ba5d, Ti4s, Ti4p etc. have been neglected in this simple picture. This may also hold for the "forbidden" transition B_{20}.

B. Comparison with Band Structure Calculations

The energies of levels L_i in Fig. 7, obtained by the procedure described above, are listed in Tables 4 and 5. These energies will now be compared with band structure calculations. By doing this one should be aware of the fact that effects due to electron hole interactions like for instance excitonic effects (see below) are neglected. This is a serious simplification, because the strong influence of excitonic effects has been established for many core level spectra (22).

As in the previous section we set the top of the valence band, TVB, equal to zero. Among the more recent band structure calculations for $SrTiO_3$ (6-8, 11), the results obtained by Mattheiss (6) seem to be most appropriate for comparison with experimental data. This calculation is based on the APW-method. The APW results for the O2s, O2p valence bands and the Ti3d lowest conduction bands have been fitted with the Slater-Koster LCAO interpolation scheme. The LCAO parameters which determine the p-d band gaps have been adjusted in accordance with optical and cyclotron-mass data. In connection with our data it is interesting that this calculation yields a direct p-d band gap, and a joint-density-of-states, which is in qualitative agreement with the low energy reflectance data (12). The adjusted LCAO band-structure shows peaks in the density of Ti3d states (DS) near energies listed in the third column of Table 4. Column four contains high symmetry points or directions in the dispersion curves, which mainly contribute to the high Ti3d DS. The agreement of peaks in the Ti3d derived density of conduction states and the energies of levels L_i, which were obtained on the basis of experimental data only, is remarkable. Therefore, the transition in Fig. 7a) can directly be correlated with high symmetry points or lines within the Brillouin zone. We want to note however that our interpretation of the structure below 10 eV is somewhat different from the one given in Ref. (12).

For the cubic and tetragonal phase of $BaTiO_3$ recent band-structure calculations have been performed by Michel-Calendini and Mesnard (9, 10). These authors use a modified LCAO method. The effects of tetragonal distortion on the energy levels is 10 - 150 meV, and will therefore be neglected henceforth. In contrast to $SrTiO_3$, these calculations yield a direct band gap at the X or Z point,

which seem to be nearly degenerate. Moreover, the Ti3d derived density of conduction states does not show peaks as pronounced as for the case of $SrTiO_3$. From the DS histogram and the dispersion curves we have tried to determine regions of "relatively" high DS. The corresponding energies are listed in the third column of Table 5. The agreement with energies of levels L_i is quite unsatisfactory. Part of the reason may be that in this calculation only Ti3d and O2p orbitals are taken into account.

C. Excitonic Effects

In the discussion given above we have focused on one electron interband transitions neglecting effects due to electron hole interactions. However, our data also show structures which most probably have to be interpreted as core excitons. The argument is as follows: From the combination of the optically determined band gap energies E_o and from the XPS data (15, 16) as compiled in Table 3 one expects the onset of core to conduction band transitions at 20.0 $\pm$ 0.1 eV for $SrTiO_3$ and at 14.4 $\pm$ 0.1 eV for $BaTiO_3$. These energies have been marked in Figs. 1 and 2. Below these onsets there are well discernible bands A_{11} and B_{11} (probably also B_{10}) for which a valence to continuum assignment is unlikely because of their relative sharpness. Therefore we attribute these peaks to the excitation of core excitons. It is an open question, whether part of the features assigned in the previous section may also be determined by core excitons associated with symmetry points higher up in the conduction bands.

V. Conclusion

Reflectivity spectra for $SrTiO_3$ and $BaTiO_3$ have been measured in the region 10 to 32 eV. Together with data of Cardona the dielectric functions were calculated. On the basis of experimental data only, most of the structures in the reflectivity curves could be explained by assuming certain energy levels L_i in the conduction band. The comparison with band structure calculations for $SrTiO_3$ did yield an excellent agreement of levels L_i and peaks in the Ti3d derived density of conduction states. For the case of $BaTiO_3$ such a good agreement was not found. The reflectivity spectra also yield evidence for core excitons.

References

(1) R. Migoni, H. Bilz and D. Bäuerle,
Phys. Rev. Lett. 37, 1155 (1976)

(2) G. Binnig and H.E. Hoenig,
Solid State Comm. 14, 597 (1974);
E.R. Pfeiffer and J.F. Schooley,
J. Low Temperature Physics 2, 333 (1970)

(3) T. Wolfram and F.J. Morin,
Appl. Phys. 8, 125 (1975)

(4) A.H. Kahn and A.J. Leyendeker,
Phys. Rev. 135, A 1321 (1964)

(5) E. Šimanek and Z. Šroubek,
Phys. Stat. Sol. 8, K47 (1965)

(6) L.F. Mattheiss,
Phys. Rev. B 6, 4718 (1972)

(7) T.F. Soules, E.J. Kelly, D.M. Vaught and J.W. Richardson,
Phys. Rev. B 6, 1519 (1972)

(8) J.D. Zook and T.N. Casselman,
Surf. Sci. 37, 244 (1973)

(9) F.M. Michel-Calendini and G. Mesnard,
Phys. Stat. Sol. 44, K 117 (1971)

(10) F.M. Michel-Calendini and G. Mesnard,
J. Phys. C 6, 1709 (1973)

(11) S. Ellialtioğlu and T. Wolfram
Phys. Rev. B 15 (1977)

(12) M. Cardona,
Phys. Rev. 140, A 651 (1965)

(13) S.K. Kurtz,
in Proc. Internatl. Meeting Ferroelectricity,
ed. by V. Dvořak, A. Fousek and P. Glogar, Prague 1966

(14) A. Frova and P.J. Boddy,
Phys. Rev. 153, 606 (1967);
M. Capizzi and A. Frova,
Phys. Rev. Letters, 25, 1298 (1970);
K.W. Blazey,
Phys. Rev. Letters, 27, 146 (1971)

(15) F.L. Battye, H. Höchst and A. Goldmann,
Solid State Comm. 19, 269 (1976)

(16) S.P. Kowalczyk, F.R. McFeely, L. Ley, V.T. Gritsyna
and D.A. Shirley, Solid State Comm. 23, 161 (1977)

(17) V. Saile, P. Gürtler, E.E. Koch, A. Kozevnikov,
M. Skibowski and W. Steinmann,
Appl. Optics 15, 2559 (1976)

(18) R. Klucker and U. Nielsen
Computer Physics Comm. 6, 187 (1973)

(19) A. Goldmann (private communication)

(20) F. Herman and S. Skillman, Atomic Structure Calculations,
Princeton, Prentice Hall (1963)

(21) W. Hayes, A.B. Kunz and E.E. Koch
J. Phys. C: Solid State Phys. 4, L 200 (1971)

(22) see. e.g. C. Kunz, Electron Hole Interaction in Deep Level
Spectra, 5 th VUV Conference, Montpellier 1977,
Journal de Physique in press.

Figure Captions

Fig. 1: Reflectivity spectra for $SrTiO_3$. Data in the energy region from 0 to 10 eV from Ref. (12). The arrow marks the expected onset of Sr4p to conduction band transitions (see text).

Fig. 2: Reflectivity spectra for $BaTiO_3$. Data in the energy region from 0 to 10 eV from Ref. (12). The arrow marks the expected onset of Ba5p to conduction band transitions.

Fig. 3: Dielectric function for $SrTiO_3$ as obtained from a Kramers-Kronig analysis of the spectrum in Fig. 1.

Fig. 4: Dielectric function for $BaTiO_3$ as obtained by a Kramers-Kronig analysis of the spectrum in Fig. 2.

Fig. 5: Optical constants for $SrTiO_3$; ——·— = loss function - Im $(\frac{1}{\varepsilon})$, ... n = real part of refractive index, ---- κ = imaginary part of refractive index, -.-.-.-. μ = absorption coefficient.

Fig. 6: Optical constants for $BaTiO_3$; ——— = loss function - Im $(\frac{1}{\varepsilon})$, ... n = real part of refractive index, ---- k = imaginary part of refractive index, -.-.-.-. μ = absorption coefficient.

Fig. 7: Energy level scheme for $SrTiO_3$ and $BaTiO_3$ as obtained from experimental data.

Table Captions

Table 1: Energies of peaks in reflection spectra of $SrTiO_3$. Labeling in parantheses and energies of A_1 to A_6 according to Ref. (12). Fundamental absorption edge, E_o, from ε_2 data in Fig. 3.

Table 2: Energies of peaks in reflection spectra of $BaTiO_3$. Labeling in parantheses and energies of B_1 to B_8 according to Refs. (12) and (14). Fundamental absorption edge, E_o, from ε_2 data in Fig. 4.

Table 3: Experimental peak energies in the density of O2p derived valence states and core level energies according to Ref. (15).

Table 4: Experimental and theoretical (6) peak energies of Ti3d derived density of conduction states in $SrTiO_3$. Last column refers to high symmetry points or lines within the Brillouin zone contributing to these peaks in the density of states.

Table 5: Experimental and theoretical (6) peak energies of Ti3d derived density of conduction states in $BaTiO_3$. Last column refers to high symmetry points or lines within the Brillouin zone contributing to these peaks in the density of states. Theoretical values according to Ref. (10).

Table 1

Energies of peaks in reflection spectra of $SrTiO_3$. Labeling in parantheses and energies of A_1 to A_6 are according to Ref. (12). The value for the fundamental absorption edge, E_o, is taken from the ε_2 data in Fig. 3 (see also Ref. 14).

Labeling	Energy (eV)	Labeling	Energy (eV)
E_o	3.4	A_9	13.0
A_1 (A_1)	4.0	A_{10}	13.8(a)
A_2 (A_2)	4.86	A_{11}	16.4(a)
A_3 (A_3)	5.5	A_{12}	19.6
A_4 (B_1)	6.52	A_{13}	20.8
A_5 (B_2)	7.4	A_{14}	21.6
A_6 (C_1)	9.2	A_{15}	22.8
A_7 (C_2)	10.2 (9.9)	A_{16}	23.4
A_8	12.0	A_{17}	24.3

(a) = these values are not included in Fig. 7

Table 2

Energies of peaks in reflection spectra of $BaTiO_3$. Labeling in parantheses and energies of B_1 to B_8 according to Ref. (12) and (14). The value for the fundamental absorption edge, E_o, is taken from ε_2 data in Fig. 4.

Labeling	Energy (eV)	Labeling	Energy (eV)
E_o	3.2	B_{13}	16.1
B_1 (A_1)	3.91	B_{14}	16.7
B_2 (A_1')	4.45	B_{15}	17.3
B_3 (A_2)	4.85	B_{16}	18.6
B_4 (A_3)	5.25	B_{17}	19.8
B_5 (B_1)	6.10	B_{18}	20.3(a)
B_6 (B_2)	7.25	B_{19}	25.2(a)
B_7 (B?)	8.1	B_{20}	27.2
B_8 (C_1)	10.3	B_{21}	30.7(a)
B_9 (C_2)	11.8		
B_{10} (D)	12.7(a)		
B_{11}	13.7(a)		
B_{12} (E)	15.1		

(a) These values are not included in Fig. 7

Table 4

$SrTiO_3$	exp. (eV)	peaks DS (Ref. (6))	
		energy (eV)	origin
L_o	3.4	3.1	$\Gamma_{25'}$, X_3, $\Delta_{2'}$
L_1	4.1	4.5	X_5, M_5, Z_2
L_2	4.9	5.1	Γ_{12}, X_2, M_3, Δ_2, $T_{2'}$, $R_{25'}$
L_3	6.5	6.2	M_1, Z_1, Σ_1
L_4	8.0	7.7	X_1, Δ_1, Z_1

Table 3

Energies (eV) of core levels and maxima (VB_i) in O2p derived density of valence states according to Ref. (15); The top of the valence bands TVB is taken as the zero for the energy scale (TVB ≙ O).

Orbital	" O2p "			Sr4p	$Ba5p_{3/2}$	$Ba5p_{1/2}$	O2s
	VB_1	VB_2	VB_3				
$SrTiO_3$	- 2.2	- 4.0	- 5.0	- 16.6	--	--	- 19.6
$BaTiO_3$	- 1.3	- 3.0	- 4.5	--	- 11.2	- 12.7	- 19.8

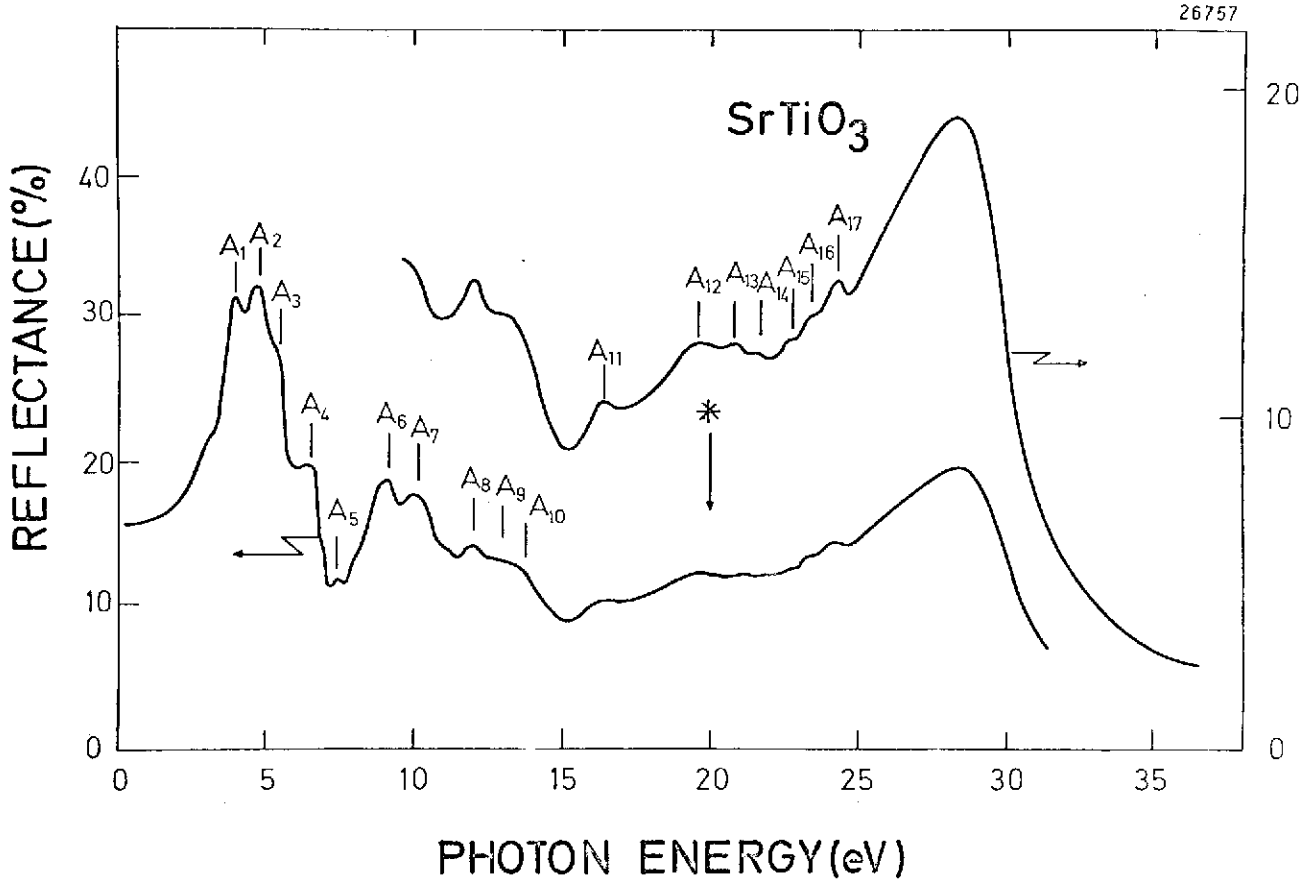

Fig. 1

Table 5

$BaTiO_3$	exp. (eV)	peaks DS (Refs. 9, 10)	
		energy (eV)	origin
--	--	2.5	X_4 , $\Gamma_{25'}$, Z_2 , Δ_2 , Λ_2
L_1	3.95	3.1	Γ_{12} , X_1 , Z_2 , Δ_1 , Λ_2
L_2	4.75	6.3	$X_{2,3}$, M_5 , R_2 , Z_5 , Y_2 , U_2 , W_2
L_3	7.3	8.4	M_1 , R_1
--	--	9.8	X_1 , M_2 , R_1 , Z_1 , Y_1 , U_1 , W_1

DESY
26759
SrTiO3
PHOTON ENERGY (eV)

Fig. 3

BaTiO3
REFLECTANCE (%)
PHOTON ENERGY(eV)
B1 B3
B4
B5
B6
B7
B8
B9
B10
B11
B12
B13
B14
B15
B16
B17
B18
B19
B20
B21
DESY
26827

Fig. 2

DESY
26820

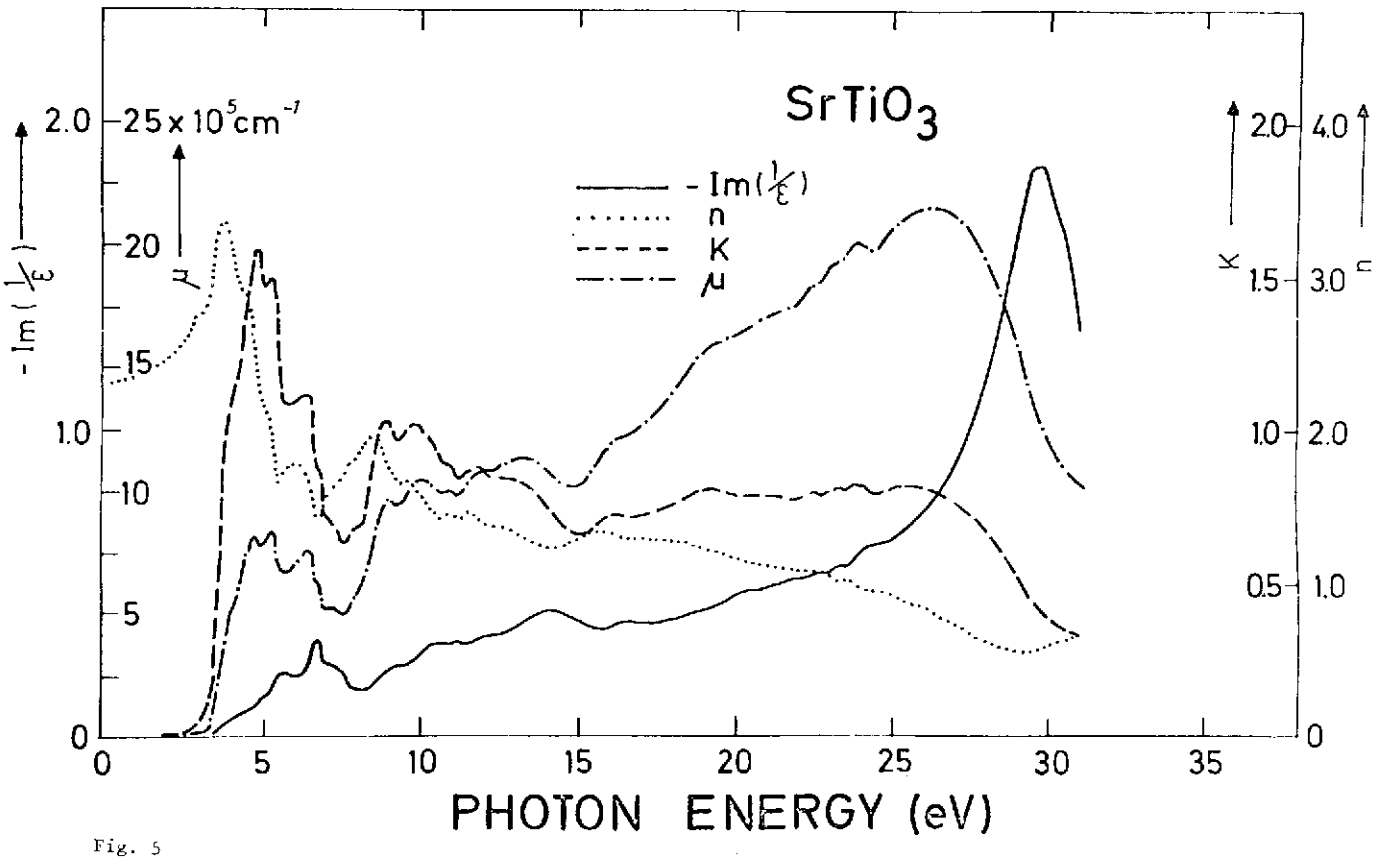

Fig. 5

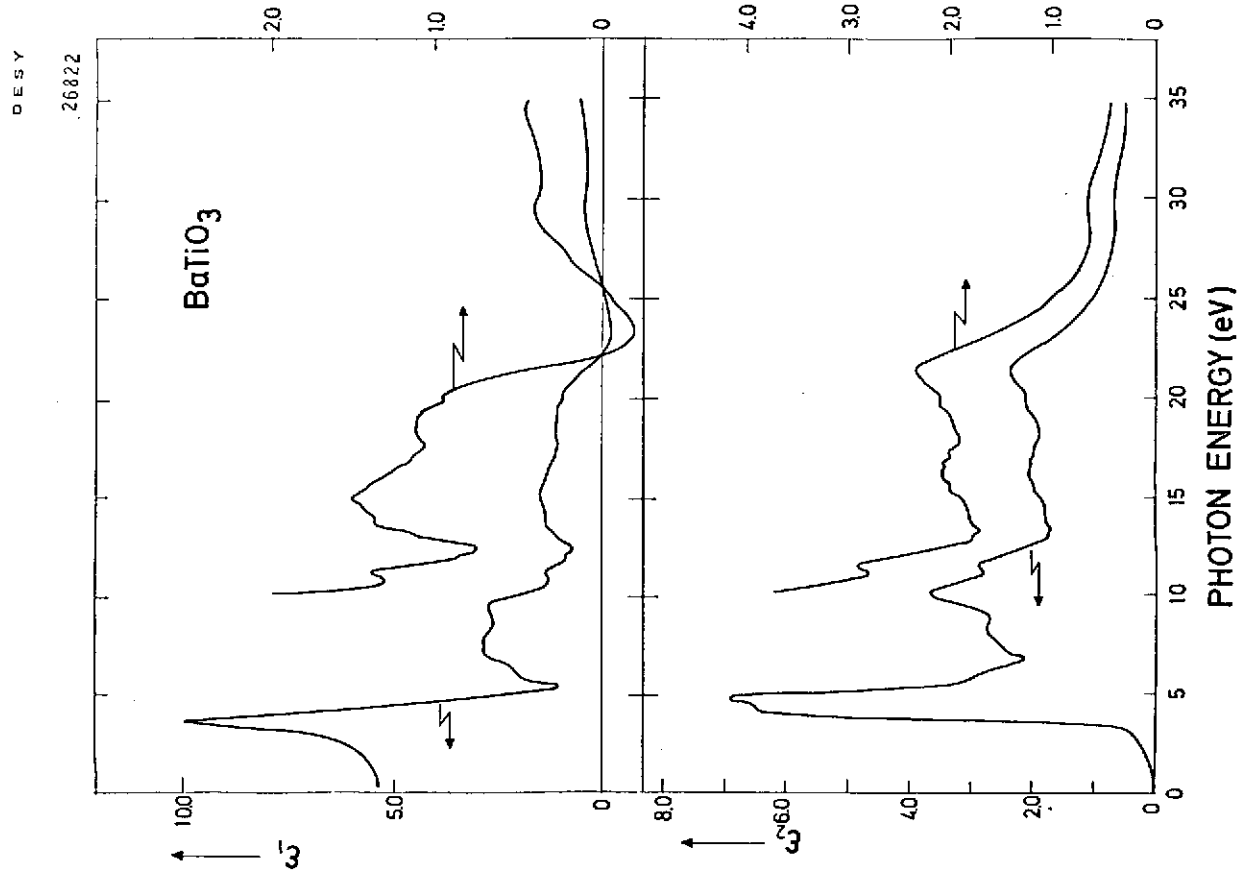

Fig. 4

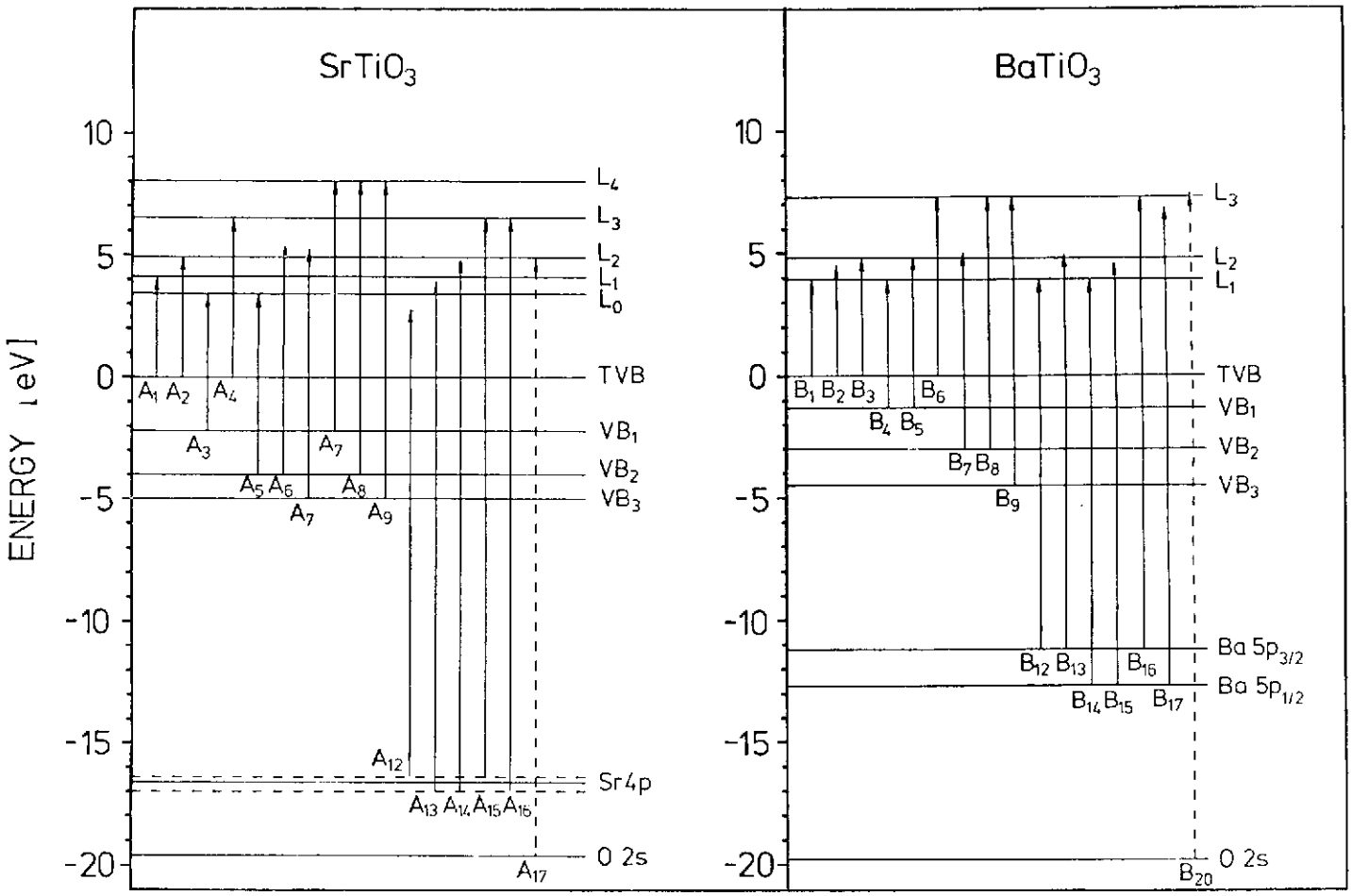
SrTiO3
BaTiO3
ENERGY (eV)
10
5
0
-5
-10
-15
-20
L4
L3
L2
L1
L0
TVB
VB1
VB2
VB3
A1 A2 A4
A3
A7
A5 A6
A8
A7
A9
A12
A13 A14 A15 A16
A17
Sr4p
O 2s
L3
L2
L1
TVB
VB1
VB2
VB3
B1 B2 B3
B6
B4 B5
B7 B8
B9
B12 B13
B16
B14 B15
B17
Ba 5p3/2
Ba 5p1/2
O 2s
B20

Fig. 7

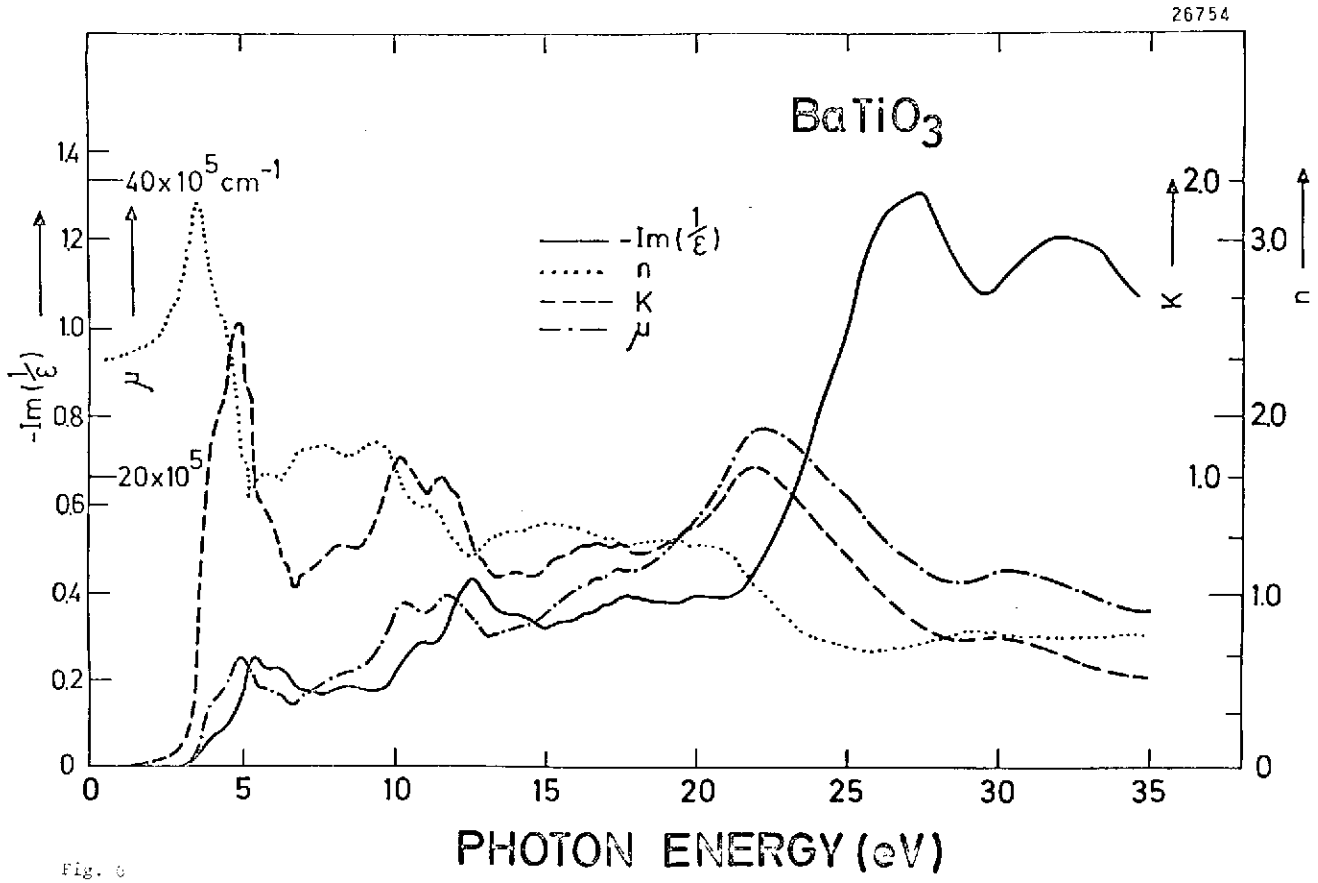
26754
BaTiO3
40x10^5 cm^-1
20x10^5
-Im(1/ε)
n
K
μ
-Im(1/ε)
μ
K
n
2.0
3.0
2.0
1.0
1.0
0
1.4
1.2
1.0
0.8
0.6
0.4
0.2
0
0
5
10
15
20
25
30
35
PHOTON ENERGY (eV)

Fig. 6